

**Accretion of Jupiter's Atmosphere from a
Supernova-Contaminated Molecular Cloud**

Submitted to Icarus 14-Oct-2008

Revised 24-Nov-2009

Accepted 9-Feb-2010

Henry B. Throop

Southwest Research Institute

1050 Walnut St, Ste 300, Boulder, CO 80302

throop@boulder.swri.edu

John Bally

Center for Astrophysics and Space Astronomy

University of Colorado, Boulder

UCB 389, Boulder, CO 80309-0389

Received _____; accepted _____

ABSTRACT

If Jupiter and the Sun both formed directly from the same well-mixed protosolar nebula, then their atmospheric compositions should be similar. However, direct sampling of Jupiter’s troposphere indicates that it is enriched in elements such as C, N, S, Ar, Kr, and Xe by 2–6× relative to the Sun (Wong *et al.* 2008). Most existing models to explain this enrichment require an extremely cold protosolar nebula which allows these heavy elements to condense, and cannot easily explain the observed variations between these species. We find that Jupiter’s atmospheric composition may be explained if the Solar System’s disk heterogeneously accretes small amounts of enriched material such as supernova ejecta from the interstellar medium during Jupiter’s formation. Our results are similar to, but substantially larger than, isotopic anomalies in terrestrial material that indicate the Solar System formed from multiple distinct reservoirs of material simultaneously with one or more nearby supernovas (*e.g.* Trinquier *et al.* 2007). Such temporal and spatial heterogeneities could have been common at the time of the Solar System’s formation, rather than the cloud having a purely well-mixed ‘solar nebula’ composition.

1. Introduction

The Solar System’s composition reflects that of the initial cloud core from which it formed. On small bodies such as the terrestrial planets, subsequent thermal and chemical processes have altered the composition. However, for the Solar System’s two largest bodies – the Sun and Jupiter (mass $1 M_J \approx 0.001 M_\odot$) – the atmospheric composition is relatively stable against change since the time of formation. In particular, the relative atmospheric

abundances of gases carbon (C), nitrogen (N), sulfur (S), argon (Ar), krypton (Kr), and xenon (Xe) are believed to be fixed at the time of formation 4.5 billion years ago, and not affected substantially by subsequent evolution. The noble gases are stable against loss due to Jupiter’s high escape velocity, and stable against sinking by condensation because they don’t combine with other atomic species. Elements C, N, and S combine into larger molecules such as CH₄, NH₃, and H₂S, but are believed to remain well mixed in Jupiter’s troposphere without settling to the interior.

Jupiter’s composition at 5–20 bars was directly measured by the Galileo descent probe’s mass spectrometer in 1995. Initial results (Atreya *et al.* 2003, hereafter AMN03) showed that Jupiter was enhanced by $\sim 3 \pm 1\times$ relative to the then-current solar abundances of Anders and Grevesse (1989, hereafter AG89). More recent work has better determined the Solar abundances, leading to revised Jupiter:Solar abundances. Somewhat surprisingly, these new results actually increased the scatter between the elements, to the broader range of $4 \pm 2\times$ (Wong *et al.* 2008, hereafter WLA08). The largest change occurred in the abundance of Jovian Ar, which more than doubled to $5.4 \pm 1.1\times$ solar (Grevesse *et al.* 2007, hereafter GAS07). A subsequent measurement of solar Ar reduces it again to $2.45 \pm 0.7\times$ (Lodders 2008)(hereafter Lod08). All enrichments in this paper are in terms of number density relative to hydrogen, normalized to the Sun; *i.e.*, $(n_i/n_H)/(n_i/n_H)_{\text{sun}}$.

2. Previous models

Several previous models have been proposed to address Jupiter’s ‘metallicity problem.’ All are based on condensation of the volatile elements into ices, which can then be concentrated relative to hydrogen. The ‘amorphous ice model’ (Owen and Encrenaz 2006; Owen *et al.* 1999) proposes that Jupiter’s atmosphere was formed from a combination of solar nebula material and ‘solar composition icy planetesimals’ (SCIPs). The SCIPs

were made of amorphous water ice in which the other volatile species condensed; these SCIPs had the same composition as the Sun, except were depleted in H. Jupiter then formed from a linear combination of these two components: when SCIPs were introduced into Jupiter from the protoplanetary disk, they were heated and released their volatiles into Jupiter’s atmosphere. (This two-component model is distinct from the formation of Jupiter’s core, which is a separate issue.) The ‘clathrate hydrate model’ (Hersant *et al.* 2008, 2004) uses a similar approach, but proposes that the volatiles are trapped within clathrate hydrates, rather than amorphous water ice. In this model, species condense out as the nebula slowly cools to their clathration temperature. The process can work at slightly warmer temperatures than the amorphous ice model. The condensation order of hydrates leads naturally to the Jovian abundance. Both models have the appeal of simplicity and directness.

These models share a common problem, that the nebula must be very cold for volatiles to condense. The condensation temperatures required are 20–35 K for the noble gases onto amorphous ice or into solids, and 35–55 K for the clathrate hydrates (Iro *et al.* 2003; Hersant *et al.* 2004). The clathrate models assume very cold nebula temperatures of <20 K at 5 AU at several Myr (Hersant *et al.* 2004). These temperatures are quite low compared with both observations and models of disks. For instance, Watson *et al.* (2007) measures 20–50 K at 50 AU, and much warmer inward, and Dutrey *et al.* (2003) measures 50 K at 100 AU. Models by Chiang and Goldreich (1997) predict 75 K at 5 AU and 55 K at 10 AU; work by Dullemond and Dominik (2005) assumes 90 K at 5 AU and 30 K at 50 AU; and the model of (Jonkheid *et al.* 2007) predicts 50 K at 100 AU. Large uncertainties exist in both observational and theoretical studies of disks, and it remains to be established that temperatures can indeed reach the low temperatures needed by these models. The low disk temperatures required are also dangerously close to the 20–50 K gas and dust temperatures of the molecular cloud itself, which set an absolute lower limit for the disk temperatures

(Johnstone and Bally 2006; Johnstone *et al.* 2006; Bally *et al.* 1991). The molecular cloud temperatures are highest in the largest clouds and those with massive stars, which are the regions most likely to be where the Solar System formed (Hester *et al.* 2004).

Several models address the temperature problem by forming solids not at their current location, but further out in the nebula (*e.g.*, 10–50 AU) where temperatures were lower. Radial migration subsequently brought them to 5 AU. For instance, Alibert *et al.* (2005) explores the possibility that Jupiter formed in its entirety at 10–15 AU via the clathrate model, and then migrated inward. Guillot and Hueso (2006) use photo-evaporation and viscous migration of the entire nebula to explain Jupiter’s enrichment. In this work, UV flux from internal and/or external stars heats and preferentially removes hydrogen from the inner proto-planetary disk. These planetesimals then migrate inward where they heat and go into forming Jupiter. This model is appealing, and consistent with the idea that the young solar system may have experienced the effects of nearby massive stars (*e.g.*, Tachibana and Huss 2003; Throop *et al.* 2001).

Bringing material from much further out, where the nebula remains cold, is appealing but there is a strong dynamical constraint on how much material from the coldest regions of the disk could be incorporated into the disk. Levison and Duncan (1997) showed that less than 0.5% of comets leaving the Kuiper Belt eventually impact Jupiter. To acquire the amount of contamination seen here would require that the Kuiper Belt have a mass on the order 2500 Earth masses. Models of Neptune’s outward radial migration to 30 AU place firm upper limits on the Kuiper belt mass of just 20 Earth masses (Gomes *et al.* 2004; Hahn and Malhotra 1999), so Jupiter likely received no more than 0.1 Earth masses of material from the Kuiper belt or beyond.

Even if the proper temperatures are somehow reached, additional problems exist for the clathrate model. Laboratory results at very low pressures are sparse and have not

shown that clathration rates at the very low nebula pressures are sufficiently fast to operate on Myr timescales (Hersant *et al.* 2008). And, in order for ice to trap other volatiles as clathrates, its surface must remain exposed (‘microscopic’ grains or cracks) for several Myr until the nebula cools (Hersant *et al.* 2004). This is inconsistent with models showing that grains grow rapidly; planetesimals up to 100 km are thought to be able to form within 1 Myr even at 30 AU (Weidenschilling 1997). If for any of these reasons clathration is inefficient, then Jupiter’s core mass could grow much higher than observed due to high O:H ratios required. Finally, this existence of such small grains would work to insulate the disk and keep it warm, rather than allow it to cool as required. Thus, the solar system’s bodies may simply have formed too large, too quickly, to clathrate sufficient volatiles from the disk atmosphere.

All the models discussed do a reasonable job of fitting Jupiter’s composition. The SCIP models predict a uniform enhancement of $3\times$ in all species, fitting the original Galileo data very well. However, no SCIPs have ever been identified in the Solar System: comets, for instance, are depleted substantially in N and are of decidedly non-SCIP composition (Iro *et al.* 2003). The clathrate models result in too much S (by a factor $2\times$). All of the models attempt to fit the roughly $3 \pm 1\times$ enhancement of the original Galileo values, and do not try to fit the newer $4 \pm 2\times$ values; Owen and Encrenaz (2006) dismisses the revised values as being possibly due to systematic errors. None of the models fit the high Ar value of $5.4 \pm 1.1\times$ of GAS07, though the 2.5 ± 0.5 value of Lod08 clearly fits more easily. Ar has in fact the *coldest* condensation temperature (~ 35 K into clathrates, and 20 K as a solid) of all the species measured, so its high GAS07 value would be a particular challenge to all the condensation models.

Finally, Lodders (2004) proposed an entirely different model: that Jupiter formed from carbon-rich (rather than ice-rich) planetesimals. However, this scenario depends on the

assumption that the Galileo probe sampled a typical region of Jupiter’s atmosphere, and most work supports the opposite view that the probe hit an anomalously dry spot.

3. Our model: A contaminated molecular cloud

We propose an entirely different solution to the problem. Rather than forming Jupiter and the Sun from identical ‘Solar nebula’ material and invoking condensation or transport within the nebula to modify Jupiter’s composition, we propose that the composition of Jupiter and the Sun differ because of intrinsic temporal and spatial variations in the Solar nebula composition as the interstellar medium (ISM) is polluted by massive stellar winds and supernovae (SNs). We show that this model can explain Jupiter’s chemical composition, easily fits into environmental formation scenarios, and is consistent with other heterogeneities in both our Solar System and distant star clusters.

In the scenario that we propose, multiple stages of star formation occurred within a giant molecular cloud (Fig. 1). The cloud was of average size, 10–20 pc, and within the GMC lay several pc-scale molecular clouds. Stars, including the Sun with its disk, began to form in clusters within these clouds. The Sun’s orbit through the cluster took it on a long path several pc across. Before any nearby O/B stars turned on, the cluster environment remained cool and dark for several Myr. During this time the Sun passed through the ISM and gravitationally swept up material onto its disk by Bondi-Hoyle accretion (Throop and Bally 2008).

If the Sun formed alone, then the composition of the ISM might be uniform. But in our proposed scenario, other clusters nearby formed a few Myr earlier, some with higher-mass stars, and the ISM surrounding these clusters soon began to be polluted in heavy elements produced by these massive stars. Nucleosynthesis in these stars enriched their ejecta by

$\sim 100\times$ or more relative to Solar H. The Sun’s evolving orbit took it through these more polluted regions of the ISM. Material was accreted onto both the Sun and its disk, but the disk’s large cross-section and low mass made it easier to pollute than the Sun. The disk’s metallicity slowly increased, and Jupiter’s core and atmosphere formed from the disk. The disk dispersed within 5–10 Myr, around the same time as the local ISM dispersed and the cluster spread apart, ejecting the Sun as an unbound field star. Jupiter’s final composition thus represented largely the same material as the Sun, but with the late accretion of polluted material reflecting in Jupiter’s enriched composition today.

Our proposed model reflects much of the current understanding of star formation in large clusters and molecular clouds (*e.g.* Bally 2008). Stars do not form in isolation, the ISM is not of uniform composition, stars travel on long orbits through their young clusters, and material from the ISM can be accreted onto young stars and disks in the several Myr after they form. All of these are newly appreciated processes that have not been incorporated into existing models of Solar System formation. We find Jupiter’s metallicity to be one natural consequence of these processes, and we explore here the issues involved with it. In the following sections we examine the detailed chemical constraints on Jupiter’s composition from such a model (§4), and the timing and spatial parameters required (§5). In §5.3 we describe several other cases where stellar pollution occurs.

4. Chemical constraints

In this section we investigate the detailed chemical enrichment from this ‘polluted accretion’ scenario and whether it can explain Jupiter’s current composition.

We start by assuming that Jupiter’s atmosphere is composed of a mixture of three distinct components. The majority of the mass is made of Solar material, whose composition

is well determined by the measurements of GAS07 and AG89. The remainder is the small amounts of pollution that come from massive stellar winds and/or supernovae. The compositions of these ejecta are distinct ‘fingerprints’ of the stars, determined mostly by their initial mass and composition. In general, the winds of these stars are enriched primarily in light elements (C, N, O, Ne), while the SN ejecta several Myr later contain heavier species (S, Ar, Kr, Xe). As one example, the demise of a star with an initial mass of $20 M_{\odot}$ can produce $5 M_{\odot}$ of O, $0.5 M_{\odot}$ of C, $0.2 M_{\odot}$ of Si, $0.001 M_{\odot}$ of ^{26}Al , and $10^{-4} M_{\odot}$ of ^{60}Fe in its SN phase (Woosley and Heger 2007, hereafter WH07). In our models, we use the grid of winds and ejecta computed by WH07. These models span the mass range 12–40 M_{\odot} , and consider a variety of nucleosynthesis rate coefficients and explosion energy parameters, for a total of 66 models.

We denote the elemental abundances in the Solar, wind, and SN components as n_{\odot} , n_{w} , and n_{sn} ; the Jupiter abundance is n_{J} . It is then possible to calculate model Jupiter compositions by using

$$n_{\text{J},i} = f_{\odot} n_{\odot,i} + f_{\text{w}} n_{\text{w},i} + f_{\text{sn}} n_{\text{sn},i}, \quad (1)$$

where i is the species and $f_{\odot} + f_{\text{sn}} + f_{\text{w}} = 1$. We use the present-day solar abundance, but the difference between this and the Sun’s primordial composition is insignificant for our purposes.

Using Eq. 1, we found combinations of solar material and ejecta that would produce Jupiter’s measured composition. We searched all $66^2 = 4356$ possible combinations of the 66 wind and 66 SN models of WH07, coupled with the single solar abundance. For each trial, we computed coefficients that best fit Jupiter. Our routine attempted to fit only the well measured stable species (C, N, S, Ar, Kr, Xe), and computed results for both these and the remaining elements (He, O, Ne, P).

Our best fit (‘Model A’) is shown in Figures 2–3. This model finds Jupiter’s composition

to be well described by 87% solar nebula, 9% stellar winds from a $40 M_{\odot}$ star (WH07’s **s40a28A**), and 4% supernova ejecta from a $20 M_{\odot}$ star (WH07’s **s20a37n**). The total contamination is 13% (*i.e.*, $0.13 M_{\text{J}}$). The fit is excellent at matching the observed quantities of C, S, Ar, and Kr, and the lower limit for O. The largest deviation is for N, where we are slightly below the error bar. The wind predominantly supplies C, N, and O while the SN supplies the remaining species. Both stars have high enough mass (and thus short enough lifetimes) that they can form and explode within the 10 Myr timeframe of GMCs. We assume the GAS07 and WLA08 values for the Solar and Jovian composition. This model is shown here because it is the best fit; many other combination of different mass SN and wind ejecta provided much worse fits.

A variant of this fit (‘Model A2’) is shown in Figures 4–5. In this case we have used the latest Lod08 value for Ar, instead of that of GAS07. This model is fit with 78% solar nebula, 8% winds from a $40 M_{\odot}$ star (WH07’s **s40a28A**), and 14% SN ejecta from a $15 M_{\odot}$ star (WH07’s **s15a34c**). The only difference to the fit is the Ar abundance. Because lower-mass SNs are less efficient at heavy-element nucleosynthesis, the fit here requires a substantially larger SN contribution than does Model A (14% vs. 4%). The $15 M_{\odot}$ star has a lifetime of ~ 11 Myr, putting it on the upper end of individual cloud lifetimes but within the timescale of large regions like Orion.

Finally, a third fit is shown in Figures 6–7 (‘Model B’). This model differs in that we have used the abundances of AG89 and AMN03 for n_{sol} and n_{Jup} . Although the newer abundances are probably preferred, using the old ones gives a test of the robustness of our fits. Also, the nucleosynthetic yields of WH07 start with the AG89 solar abundances, so in a sense this fit is more self-consistent, even though it is based on slightly older data. Model B requires about 6% total contamination, less than half that required by Model A. Model B is comprised of 94% solar, 4% stellar winds from a $40 M_{\odot}$ star (**s40a28A**), and 1.5% SN

ejecta from a $25 M_{\odot}$ star (s25a41d).

All three of our models fit the data well. In all cases the vast majority of Jupiter’s mass (78%-95%) comes from the Solar nebula, in agreement with standard models. And in each, a combination of winds and SN – which one would expect in a realistic cluster – works better than any single component by itself. All three fits are slightly low in N and Xe; the remaining species are fit very well.

The individual ‘fingerprints’ of the SNs can be seen in Figures 7, 5, and 3. In all the models, the lighter species (C, N, O) are produced in the winds, while the heavier elements come from the SNs and are highly dependent on the SN mass. A large difference between the three models is the SN C:N ratio, which is several times higher in Model B than the others (compare red curves in 5 and 3). The great deal of carbon ejected by the Model B SN allows the total contamination in this model to be about half that in Model A.

Detailed yields from our three models are listed in Table 1. This table lists additional species measured by Galileo, but which are not in equilibrium at the entry site and thus not expected to fit: He, Ne, and P. Helium and Ne are believed to combine into He-Ne ‘raindrops’ which sink to Jupiter’s interior, and cannot be used as a constraint (Roulston and Stevenson 1995). Helium itself is produced by the Sun so its primordial Solar abundance cannot be directly measured. O was measured at Jupiter but its value is believed to be anomalously low due to the probe’s dry entry site. Encouragingly, our models predict primordial Jovian abundances for O, Ne, and P similar to those of the other species. The predicted values for O are in the range 2.6–2.9, similar to global O values determined spectroscopically (WLA08).

Several changes could improve the quality of our fits. First, we have used a simple fitting method, assuming contamination by only one wind and one supernova. In realistic star-forming regions such as Orion there are several dozen stars within a few pc all above

$8 M_{\odot}$ that will explode as SN; using multiple stars will increase the ease of fitting Jupiter’s composition. Second, the SN ejecta models we use are quantized in relatively large mass bins ($5 M_{\odot}$), and all use certain common assumptions for stellar and explosion parameters. The SN ejecta yields are very model dependent; for instance, the models of Young and Fryer (2007) vary in abundance for individual species by 50% or more from those of WH07 for stars of similar mass. The WH07 yields ignore stellar rotation, which may be important (Hirschi *et al.* 2005). Thus, a better understanding of SN yields could help (or hurt) our fits. Finally, we have not included physical processes in the ISM or disk such as sedimentation, concentration, or condensation, even though these could be important. For instance, of the noble gases our poorest fit is for Xe, which is low by 50% and at the edge of the 1σ error bar. However, Xe condenses at a substantially warmer temperature than any of the other noble gases (at ~ 55 K into clathrates, it is the easiest to condense), so if our model were to include condensation explicitly, it would operate in the direction to correct this deficiency. For now, however, we have intentionally chosen to keep our models simple to demonstrate that good fits are possible even with a very limited set of parameters.

5. Stellar Pollution into the ISM

Now that we have shown that Jupiter can be matched chemically, we investigate the requirements on the environment to support such contamination.

As massive stars in a cluster evolve, they perform nucleosynthesis and create heavy elements that pollute the ISM. These are given off in stellar winds (during the stellar lifetime) or SNs (at the end-of-life for stars with $M > 8 M_{\odot}$). After being injected into the ISM, these highly enriched ejecta are incorporated into the next generation of stars. The highest-mass stars are the shortest lived: for instance, the $40 M_{\odot}$ stars used in our fits explode in less than 5 Myr, allowing for a full generation of star formation within the

10 Myr timescales of planet formation and embedded clusters.

5.1. Contamination by Stellar Winds

Stars spend the majority of their lives on the main sequence. During this stage the stellar winds are weak enough that they do not pollute the cluster; for instance, the current solar wind is $\dot{M}_{\odot} \approx 2 \times 10^{-14} M_{\odot} \text{ yr}^{-1}$ with $v \approx 400 \text{ km s}^{-1}$. Red supergiant (RSG) stars, however, have slow massive winds that can easily pollute the cluster. RSGs are normal post-main-sequence stars of mass 5–15 M_{\odot} that have cooled dramatically after their main-sequence phase ($T > 10,000 \text{ K}$ to $T < 3000 \text{ K}$), and have heavy and slow winds of $\dot{M} \approx 10^{-5}$ – $10^{-4} M_{\odot} \text{ yr}^{-1}$ and v as low as 10 km s^{-1} – *ten order of magnitude* more loss than the present-day Sun (Knapp and Woodhams 1993). The RSG phase lasts for 5–10% of the stellar lifetime, or typically a few 10^5 – 10^6 yr (Schaller *et al.* 1992). For stars $> 25 M_{\odot}$, over half the original stellar mass can be lost during the RSG phase (Garcia-Segura *et al.* 1996). The wind velocity of 10 km s^{-1} is only slightly higher than the stellar and gas velocities, so this material can readily mix with the local ISM. The abundances n_w that we consider in § 4 are predominantly from the RSG phase, because stars of less than $20 M_{\odot}$ evolve too slowly ($> 10 \text{ Myr}$) to enter the RSG phase within typical cluster lifetimes. Our Model A and B fits use winds from stars of $40 M_{\odot}$ with lifetimes $\sim 5 \text{ Myr}$, which easily fit the timing constraints. These high-mass stars are seen in clusters of $N >$ a few thousand; an example is $\theta^1 \text{ Ori C}$ in the Orion Trapezium core. Smaller $8 M_{\odot}$ stars are produced in clusters of $N >$ a few hundred.

5.2. Contamination by Supernova Ejecta

After passing through the RSG phase, stars with masses $> 8 M_{\odot}$ usually end their lives as SNs. The SN explosion gives off $1\text{--}5 M_{\odot}$ of metal-enriched material at speeds of $2,000\text{--}10,000 \text{ km s}^{-1}$. Even at such high speeds, numerical simulations by Ouellette *et al.* (2007) showed that disks at 1 pc are very resilient to nearby explosions. However, although the disk will absorb most of the intercepted solids such as ^{60}Fe , most of the SN’s gas is deflected by the disk. For a $20 M_{\odot}$ explosion at 1 pc, the disk will absorb just $10^{-4} M_{\text{J}}$ of enriched gas, insufficient for the process described here.

But, there are at least two mechanisms by which ejecta may cool and then be accreted onto the disk. First, as the ejecta spreads, it mixes with the ISM until it slows and cools, and this cooler ejecta can be accreted more easily. In order to slow to 10 km s^{-1} , $1 M_{\odot}$ of SN ejecta must mix with roughly $1000 M_{\odot}$ of ISM (*i.e.*, a 1000:1 mixing ratio). The SN ejecta can be quite clumpy, with high mixing ratios in some regions and low in others. Rather than mixing uniformly, these clumps appear to be slowed as a unit and preserve their density, much like a baseball is slowed in the air without fully mixing. Observations of pc-scale ejecta from various SNs show highly clumpy knots on AU scales or greater maintained for a year after explosion (Fesen *et al.* 2007; Wang and Hu 1994). Observations of emission lines even 700 years after the explosion continue to find evidence for density contrasts of 100–200 in dense metal-rich bubbles within the ejecta (Williams *et al.* 2008; Fesen *et al.* 2006). Additional work shows that some heterogeneity persists on even longer Myr timescales (Freyer *et al.* 2006; Kroeger *et al.* 2006). Thus, diluting to a 1000:1 mixing ratio is needed to slow the material, there will likely be local regions where the mixing ratio could be 100:1 or lower, roughly the amount of SN pollution required by our ‘Model B’ case. The GMC itself is generally robust against disruption by SNs, as evidenced by the Orion region, which has seen dozens of supernovae in the past 12 Myr (Bally 2008), yet

remains largely a cool GMC.

The second mechanism involves AU-scale ‘droplets’ of ejecta that can travel from a supernova exploding as a ‘champagne fountain,’ through the ISM, and land cool and intact in molecular clouds many kpc distant. This mechanism is believed to be responsible for observed compositional heterogeneities (‘abundance discrepancy factors’, or ADFs) of 50%–10 \times in molecular clouds (Mesa-Delgado *et al.* 2008; Stasinska *et al.* 2007; Tsamis and Pequignot 2005; Tenorio-Tagle 1996). These ADFs are seen in cold, dense, hydrogen-depleted gaseous regions in the middle of larger molecular clouds, on scales of 10–100 AU. They are commonly seen in star-forming clouds including Orion and 30 Doradus. The droplets have mixing lifetimes of several Myr, consistent with the timescales needed for our Jupiter model. In this way, dense concentrations of gaseous metals produced by the SN are transported to and preserved in the nebula, where they are then passed on to stars and planets that form in the region (Stasinska *et al.* 2007).

5.3. Accretion of the ISM onto disks

Once enriched material has mixed with the ISM by either of these two methods, accretion onto the disk is straightforward. Throop and Bally (2008) found that the average ISM-to-disk accretion rate for disks in young clusters was $10^{-8} M_{\odot} \text{ yr}^{-1}$, or ~ 1 MMSN per Myr. The total accretion needed in our Model B case is $0.1 M_J = 10^{-2} \text{ MMSN} = 10^{-4} M_{\odot}$, or the amount delivered in $\sim 10,000$ years. Since accretion may be maintained for 5 Myr, this provides more than sufficient mass delivery. Due to the disk’s large cross-section and its low mass, accretion affects the disk but makes only negligible effect on the stellar composition (Moeckel and Throop 2009).

6. Heterogeneity in the Solar System and star-forming regions

Our model reflects the growing body of evidence that the Solar System did not form from a homogeneous cloud in an isolated environment, but rather from a heterogeneous nebula where interactions with its environment played a major role in shaping its evolution. We briefly discuss here four examples of large-scale heterogeneity: two in the terrestrial planets, one in star-forming regions, and one on galactic scales.

The terrestrial bodies have been modified by scores of chemical and physical processes since their formation. Most of these processes act equally on all isotopes of the same element, so isotopic differences are not expected in samples formed from a well-mixed nebula. However, isotopic variations *have* indeed been measured in samples from the Earth, Mars, and numerous asteroids. Isotopic differences have been measured for species including Ba, Cr, S, Ti, Zr, Nb, O, and more (Trinquier *et al.* 2007; Ranen and Jacobsen 2006; Dauphas *et al.* 2002, and references therein). These anomalies are small (up to 1% for $^{54}\text{Cr}/^{53}\text{Cr}$, and as small as ppm for some others) but are indisputable. UV photochemistry has been invoked to explain the origin of the O variations (Lyons and Young 2005), but the remaining heterogeneities have defied explanation by known fractionation processes. Instead, they are consistently thought to be of nucleosynthetic origin, resulting from the incomplete mixing of ejecta from multiple SNe in the material of the young solar nebula (Ranen and Jacobsen 2008; Trinquier *et al.* 2007; Ranen and Jacobsen 2006; Dauphas *et al.* 2002).

In addition to the stable isotopes, variations have been found in short-lived radioactive isotopes, allowing some constraint on the timing of the Solar System’s early heterogeneity. Krot *et al.* (2008) examined the heterogeneity of ^{26}Al isotopes within Ca-Al inclusions (CAIs) in carbonaceous chondrites. They found differences of $> 100\times$ in primordial ^{26}Al abundances, leading to the conclusion that there are at least two populations of CAIs:

some which were formed in the presence of ^{26}Al , and some which were not. This requires either spatial or temporal variations in the Solar System birth environment. Their preferred interpretation is that the ^{26}Al -free CAIs were formed early (possibly during initial collapse of the Solar System), followed by late injection of ^{26}Al from a nearby massive star. They suggested that this massive star could be the same one that injected ^{60}Fe several Myr later after an SN explosion. We caveat this point with mention that a recent study of CAIs within a single ordinary chondrite did not reproduce the ^{26}Al variations (Villeneuve *et al.* 2009); it is possible there are regions that were heterogeneous and regions that were not.

Orion, the nearest massive star-forming region, shows evidence for ‘polluted accretion’ amongst individual young stars. Observations of the metallicity of 29 B, F, and G stars within Orion have found abundance variations up to $4\times$ between stars of the same age in the same subgroup (Cunha *et al.* 2000, 1998; Cunha and Lambert 1994). These variations are spatially correlated, suggesting that recent supernovae have contaminated distinct regions of the cluster. The abundance variations are seen in O and Si (which are produced by massive stars and type II SNs), but not in Fe, C, and N (which are produced to a far lesser degree, and thus would not be expected to contaminate the stars). The authors proposed that ejecta from recent SNs have been accreted onto these stars, causing their observed metallicity.

Relative to the galactic value, the entire Solar System exhibits a system-wide excess of 30% in $^{18}\text{O}/^{17}\text{O}$, and the solar value is higher than nearly every molecular cloud or YSO within 10 kpc. This enhancement has been proposed to be due to accretion of supernova ejecta and massive stellar winds immediately prior to the proto-Solar nebula’s formation (Young *et al.* 2009, 2008).

These four examples describe heterogeneity broadly similar to what we propose for Jupiter. The contamination at Jupiter is many times higher than the isotopic anomalies in

the terrestrial bodies. However, the terrestrial anomalies were formed earlier in the solar system’s history, over a shorter period, and in a warmer and better-mixed region. Jupiter formed later and in the outer solar system, where chemical pollution can more easily be acquired from the ISM, and mixing times are far longer. While the small terrestrial anomalies were likely to have been inherited from incomplete mixing of the *initial* solar nebula, Jupiter’s enhancement could be caused by *post-collapse* contamination of the disk, from Bondi-Hoyle accretion onto the disk over several Myr and several pc, allowing for far more introduced pollution across the entire molecular cloud. The amount of heterogeneity seen at Jupiter *is* comparable or smaller than that seen in both star-forming regions (ADFs) and young stars themselves. Because the physical processes of star formation are universal, if the Sun formed in a dense cluster, then the solar system and Jupiter could have naturally inherited these heterogeneities.

7. Discussion

The model we propose here is a departure from existing models for the solution to Jupiter’s metallicity problem. Although historically most Solar System formation models have assumed a homogeneous ‘Solar nebula’ composition, our model explicitly assumes the opposite. We incorporate the fact that the composition of the solar nebula can change spatially and temporally. These changes occur during the Solar System’s first 5–10 Myr, as the Sun is traveling through its birth cloud, experiencing the environmental effects of other stars. The inclusion of this contamination reflects the latest understandings of the environmental processes affecting star formation.

Our model has three general advantages over the existing amorphous ice and clathrate models that we describe in § 2. First, it relaxes the very strict low-temperature requirements for the formation of Jupiter’s solids. Second, it allows for Jupiter to have formed at its

present location without migration. Third, it explains the fact that different elements are enriched by different amounts (*i.e.*, not a uniform $3\times$).

Our model is not without problems. Our fits for N are at the edge (or a little beyond) the 1σ level. Nitrogen is poorly measured in the Galileo probe data, but is a major species and an important constraint. We could increase the contribution from stellar winds (which supply much of the N), but this would increase the amount of C beyond that observed. Low-mass stars of $4\text{--}8 M_{\odot}$ produce large quantities of N sufficient to solve the problem, but these stars have lifetimes of 30 Myr or more before they enter the RSG phase. The other specie our models are all low in, Xe, has a particularly high condensation temperature (making it easy to condense), and this may in part explain its abundance.

Second, the amount of SN contamination required is on the high end of what can be supplied by nearby SNs using direct injection of ejecta into a nearby GMC. Additional work is necessary to understand the mixing and concentration mechanisms of this ejecta. However, if the ‘droplet’ model of SN ejecta is correct, then concentrated ejecta can be slowed and cooled over kpc distances, which would solve this problem.

Most work suggests that Saturn, Uranus, and Neptune accreted their atmospheres from the disk in much the same way Jupiter did. The metallicity enrichments of the outer planets exceed Jupiter’s – Uranus and Neptune have 30 times the Solar C:H ratio, for instance – suggesting that they were formed at least in part by the traditional chemical condensation series (Lewis 1972). The colder nebula and slower evolution make volatile condensation easier at greater distances. However, ‘accreted pollution’ of the disk from the ISM would affect these planets as well. Because of their different positions in the disk and their different formation times, our model cannot *predict* the enrichment they may receive from pollution, except that it could be similar to Jupiter’s. (The outer disk, with its larger cross-section, might be more easily contaminated, but this requires more study.) More

detailed analysis of this awaits better knowledge of their bulk atmospheric compositions, which are largely unknown today. Jupiter’s oxygen composition will be probed by Juno in 2017 and will provide a discriminant between many models including our own (which predicts a global O:H ratio of $\sim 2.6\times$ solar) and that of Lodders 2004 (which assumes $\sim 0.35\times$ solar).

Jupiter’s atmosphere may have formed through a variety of processes, of which polluted accretion could be only one. For instance, N is among the most difficult species to condense in the various ice models, as it requires a temperature ≤ 30 K. Nitrogen, however, is easily supplied in the cool, slow stellar winds that we study here. It is possible that N was supplied by these winds, and other species were delivered in part by icy planetesimals from a relatively warm (≥ 50 K) disk.

An advantage of the SN model is that it provides a mechanism for matching not only the chemical abundances which we study here, but also isotopic differences. It has already been shown that SNs may explain the isotopic differences seen in the Solar System’s rocky bodies (§ 6); additional work on the isotopic differences between the Sun and Jupiter would be a natural extension of the present work. This path is particularly ripe for future study given the recent Solar composition results from the Genesis mission (*e.g.*, Wiens *et al.* 2007; Mabry *et al.* 2007).

The general process of accretion from ISM \rightarrow disk \rightarrow planet that we describe here has broader applications for the formation of extrasolar planets. A strong observed correlation exists between the metallicity of the host star and the existence of extrasolar planets (*e.g.*, Udry *et al.* 2007). We predict that the correlation between stellar and planet metallicities will depend on the formation environment. Stars that form in dense regions, in the presence of massive stars, will have the highest disk metallicities and thus the greatest chance of forming planets.

8. Acknowledgments

We thank S. Atreya, W. Bottke, F. Ciesla, A. Heger, T. von Hippel, H. Levison, A. Morbidelli, and M. Wong for useful discussions. Heger and S. Woosley also kindly provided the ejecta compositional data which we use here. HT and JB graciously acknowledge support from NASA Origins grants NNG06GH33G and NNG05GI43G; HT acknowledges support from NASA Exobiology grant NNG05GN70G, and JB acknowledges support from the University of Colorado Center for Astrobiology, which is supported by the NASA Astrobiology Institute.

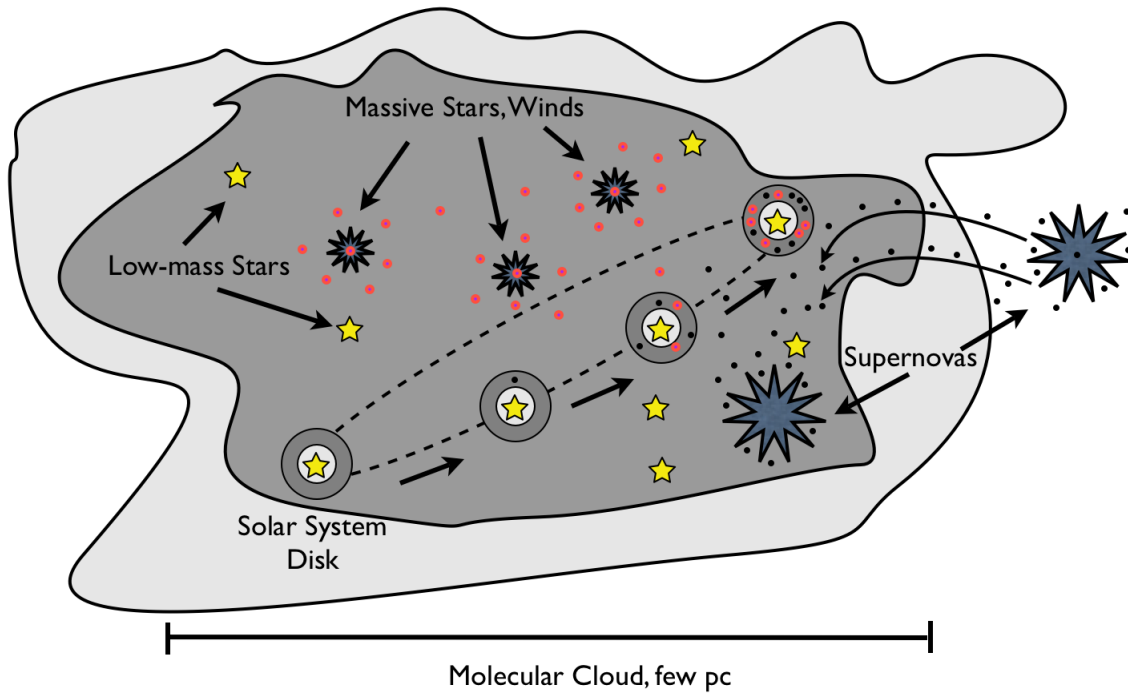


Fig. 1.— The proposed ‘polluted accretion’ scenario for Jupiter’s atmosphere. In this model, the Sun and its disk form in a low-metallicity molecular cloud (left). The Sun’s orbit takes it through other regions (right) of higher metallicity, polluted by massive stellar winds and supernovae. Ongoing Bondi-Hoyle accretion from the ISM delivers this enriched material to the disk, where it is incorporated into Jupiter’s atmosphere.

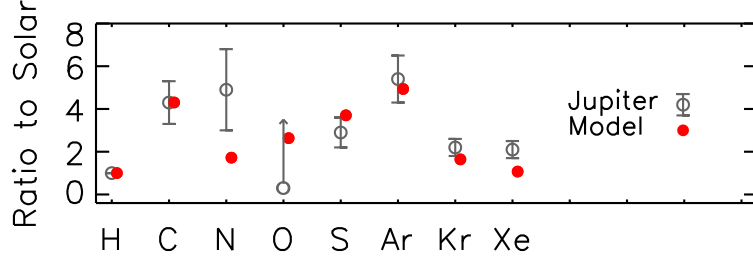


Fig. 2.— Elemental abundances of Jupiter from Galileo probe (grey), and fits for our ‘Model A’ case (red). The y axis plots the elemental number abundances relative to the Solar abundances, normalized to hydrogen. The model consists of a linear combination of 87% solar composition, 9% from stellar winds from a $40 M_{\odot}$ star, and 4% ejecta from an SN of original mass $20 M_{\odot}$. O is a lower limit because the Galileo probe entered Jupiter at a cloud-free location believed to be anomalously dry. Solar and Jupiter compositions are revised 2007 values (GAS07, WLA08).

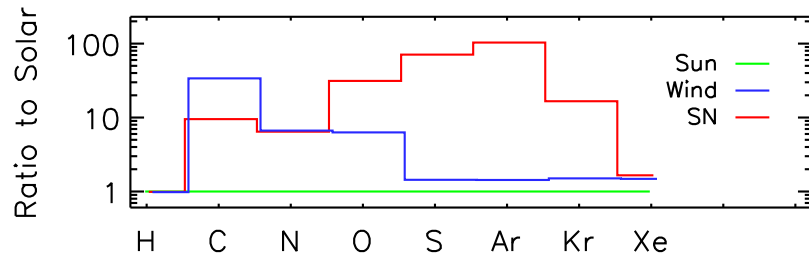


Fig. 3.— Sources of individual species in our ‘Model A’ case. The model is a linear combination of elemental abundances from the Sun (green curve), stellar winds (blue curve), and an SN (red curve). Each line is normalized to H at 1.0. The stellar winds produce much of the C and N, while the supernova supplies most of the remaining species.

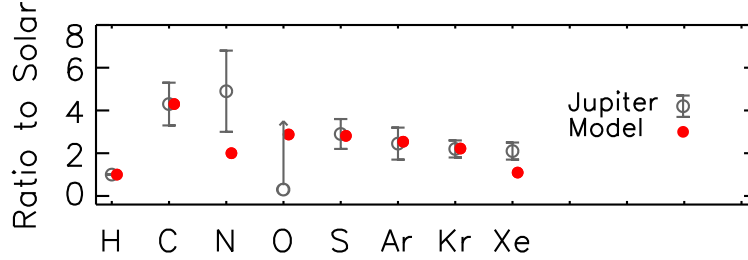


Fig. 4.— Elemental abundances of Jupiter from Galileo probe (grey), and fits for our ‘Model A2’ case (red). The model consists of a linear combination of 78% solar composition, 8% from stellar winds from a $40 M_{\odot}$ star, and 14% ejecta from an SN of original mass $20 M_{\odot}$. Abundances are the same as Model A, except the Lod08 argon value is used.

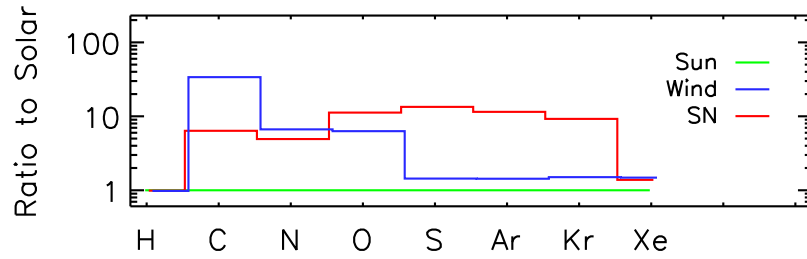


Fig. 5.— Sources of individual species in our ‘Model A2’ case. Same as Figure 3, but using Lod08 argon value.

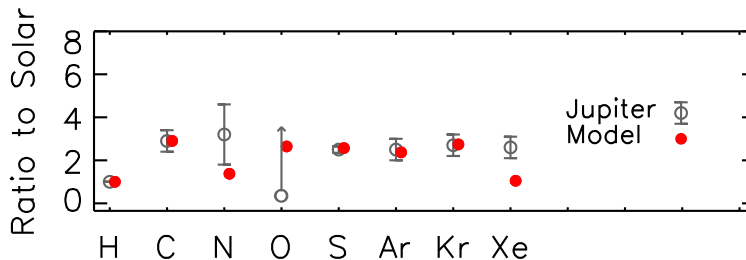


Fig. 6.— Our ‘Model B’ fits. Same as Figure 2, but assuming 1989 solar composition data (AMN03, AG89). The coefficients are Solar (94%), stellar winds from $40 M_{\odot}$ star (4%), and a supernova from a star of original mass $25 M_{\odot}$ (1.5%). The fractional contamination in this model is 6%, less than half that in Model A. The low predicted value for Xe might be explained by its particularly high condensation temperature (see text). The broad similarity of the results to the ‘Model A’ case shows that our model is robust against small changes to knowledge of the composition of the Sun and Jupiter.

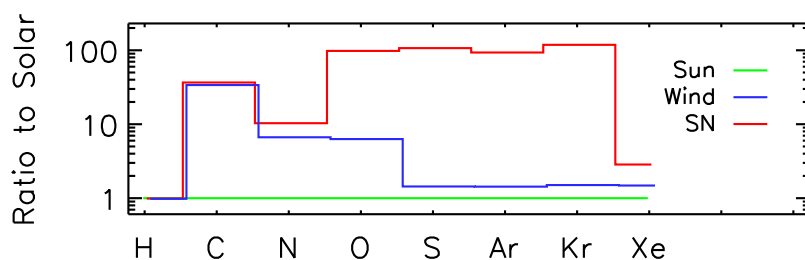


Fig. 7.— Individual components of our ‘Model B’ fits. Same as Figure 3, but using 1989 solar abundances (AMN03, AG89).

		Model A				Model A2				Model B			
Species	Sun	Wind	SN	Tot	Jupiter	Wind	SN	Tot	Jupiter	Wind	SN	Tot	Jupiter
✓= Stable		9%	4%		WLA08	8%	14%		WLA08+Lod08	4%	1%		AMN03
H ✓	1.0	1.0	1.0	1.0	1.0	1.0	1.0	1.0	1.0	1.0	1.0	1.0	1.0
He	1.0	2.1	2.3	1.2	0.8 ± 0.0	2.1	1.9	1.2	0.8 ± 0.0	2.1	3.7	1.1	0.8 ± 0.0
C ✓	1.0	33.9	9.5	4.3	4.3 ± 1	33.9	6.4	4.3	4.3 ± 1	33.9	36.6	2.9	2.9 ± 0.5
N ✓	1.0	6.7	6.5	1.7	4.9 ± 1.9	6.7	4.9	2.0	4.9 ± 1.9	6.7	10.3	1.4	3.2 ± 1.4
O	1.0	6.3	31.3	2.6	0.3 ± 0.2	6.3	11.3	2.9	0.3 ± 0.2	6.3	98.1	2.6	0.3 ± 0.2
Ne	1.0	3.7	6.7	1.5	0.1 ± 0.1	3.7	9.9	2.5	0.1 ± 0.1	3.7	90.9	2.4	0.1 ± 0.0
P	1.0	1.6	170.0	7.5	0.8 ± 0.0	1.6	17.6	3.4	0.8 ± 0.0	1.6	139.9	3.1	0.8 ± 0
S ✓	1.0	1.5	71.0	3.7	2.9 ± 0.7	1.5	13.4	2.8	2.9 ± 0.7	1.5	106.9	2.6	2.5 ± 0.15
Ar ✓	1.0	1.5	103.4	4.9	5.4 ± 1.1	1.5	11.5	2.5	2.5 ± 0.7	1.5	93.3	2.4	2.5 ± 0.5
Kr ✓	1.0	1.5	16.6	1.6	2.2 ± 0.4	1.5	9.2	2.2	2.2 ± 0.4	1.5	118.4	2.7	2.7 ± 0.5
Xe ✓	1.0	1.5	1.7	1.1	2.1 ± 0.4	1.5	1.4	1.1	2.1 ± 0.4	1.5	2.9	1.1	2.6 ± 0.5

Table 1: Details of model results, based on the listed ejecta yields from winds and SN compared with Jupiter. Table lists species observed by Galileo; abundances are in number density relative to H, normalized to Solar. The checked species are those which are stable at Jupiter and our model attempts to fit; we predict the unchecked species but do not attempt to fit them. The three models are based on different measurements for the Jupiter:Solar abundances.

REFERENCES

- Alibert, Y., O. Mousis, and W. Benz, 2005, On the volatile enrichments and composition of Jupiter. *Astrophys. J.* **622**, L145–L148.
- Anders, E. and N. Grevesse, 1989, Abundances of the elements: meteoritic and solar. *Geochimica et Cosmochimica Acta* **53**, 197–214.
- Atreya, S. K., P. R. Mahaffy, H. B. Niemann, M. H. Wong, and T. C. Owen, 2003, Composition and origin of the atmosphere of Jupiter – an update, and implications for the extrasolar giant planets. *Plan. Spac. Sci.* **51**, 105–112.
- Bally, J., 2008, Overview of the Orion complex. In *Handbook of Star Forming Regions* (ed. B. Reipurth), ASP Conf. Series, Astron. Soc. Pac., San Francisco.
- Bally, J., W. D. Langer, and W. Liu, 1991, Infrared dust and mm-wave CO emission in the Orion region. *Astrophys. J.* **383**, 645–663.
- Chiang, E. I. and P. Goldreich, 1997, Spectral energy distributions of T Tauri stars with passive circumstellar disks. *Astrophys. J.* **490**, 368–376.
- Cunha, K. and D. L. Lambert, 1994, Chemical evolution of the Orion association. II. The carbon, nitrogen, oxygen, silicon, and iron abundances of main-sequence B stars. *Astrophys. J.* **426**, 170–191.
- Cunha, K., V. V. Smith, and D. L. Lambert, 1998, Chemical evolution of the Orion association. IV. The oxygen and iron abundances of F and G stars. *Astrophys. J.* **493**, 195–205.
- Cunha, K., V. V. Smith, E. Parizot, and D. L. Lambert, 2000, Light-element abundance patterns in the Orion association. I. Hubble Space Telescope observations of boron in G dwarfs. *Astrophys. J.* **543**, 850–860.

- Dauphas, N., B. Marty, and L. Reisberg, 2002, Molybdenum evidence for inherited planetary scale isotope heterogeneity of the protosolar nebula. *Astrophys. J.* **565**, 640–644.
- Dullemond, C. P. and C. Dominik, 2005, Dust coagulation in protoplanetary disks: A rapid depletion of small grains. *Astron. & Astrophys.* **434**, 971–986.
- Dutrey, A., S. Guilloteau, and M. Simon, 2003, The BP Tau disk: a missing link between Class II and III objects? *Astron. & Astrophys.* **402**, 1003–1011.
- Fesen, R. A., M. C. Hammell, J. Morse, R. A. Chevalier, K. J. Borkowski, M. A. Dopita, C. L. Gerardy, S. S. Lawrence, J. C. Raymond, and S. van den Bergh, 2006, The expansion asymmetry and age of the Cassiopeia A supernova remnant. *Astrophys. J.* **645**, 283–292.
- Fesen, R. A., P. A. Hoefflich, A. J. S. Hamilton, M. C. Hammell, C. L. Gerardy, A. M. Khokhlov, and J. C. Wheeler, 2007, The chemical distribution in a subluminous type Ia supernova: Hubble Space Telescope images of the SN 1885 remnant. *Astrophys. J.* **658**, 396–409.
- Freyer, T., G. Hensler, and H. W. Yorke, 2006, Massive stars and the energy balance of the interstellar medium. II. The $35 M_{\odot}$ star and a solution to the ‘missing wind problem’. *Astrophys. J.* **638**, 262–280.
- Garcia-Segura, G., N. Langer, and M.-M. Mac Low, 1996, The hydrodynamic evolution of circumstellar gas around massive stars. II. The impact of the time sequence O star \rightarrow RSG \rightarrow WR star. *Astron. & Astrophys.* **316**, 133–146.
- Gomes, R. S., A. Morbidelli, and H. F. Levison, 2004, Planetary migration in a planetesimal disk: why did Neptune stop at 30 AU? *Icarus* **170**, 492–507.

- Grevesse, N., M. Asplund, and A. J. Sauval, 2007, The solar chemical composition. *Space Sci. Rev.* **130**, 105–114.
- Guillot, T. and R. Hueso, 2006, The composition of Jupiter: sign of a (relatively) late formation in a chemically evolved protosolar disk. *Month. Not. Royal Astron. Soc.* **367**, L47–L51.
- Hahn, J. M. and R. Malhotra, 1999, Orbital evolution of planets embedded in a planetesimal disk. *Astron. J.* **117**, 3041–3053.
- Hersant, F., D. Gautier, and J. I. Lunine, 2004, Enrichment in volatiles in the giant planets of the Solar System. *Plan. Spac. Sci.* **52**, 623–641.
- Hersant, F., D. Gautier, G. Tobie, and J. I. Lunine, 2008, Interpretation of the carbon abundance in Saturn measured by Cassini. *Plan. Spac. Sci.* **56**, 1103–1111.
- Hester, J. J., S. J. Desch, K. R. Healy, and L. A. Leshin, 2004, Perspectives: The cradle of the solar system. *Science* **304**, 1116–1117.
- Hirschi, R., G. Meynet, and A. Maeder, 2005, Yields of rotating stars at solar metallicity. *Astron. & Astrophys.* **433**, 1013.
- Iro, N., D. Gautier, F. Hersant, D. Bockelee-Morvan, and J. I. Lunine, 2003, An interpretation of the nitrogen deficiency in comets. *Icarus* **161**, 511–532.
- Johnstone, D. and J. Bally, 2006, Large-area mapping at 850 μm . V. Analysis of the clump distribution in the Orion A South molecular cloud. *Astrophys. J.* **653**, 383–397.
- Johnstone, D., H. Matthews, and G. F. Mitchell, 2006, Large area mapping at 850 micron. IV. Analysis of the clump distribution in the Orion B South molecular cloud. *Astron. J.* **639**, 259–274.

- Jonkheid, B., C. P. Dullemond, M. R. Hogerheijde, and , 2007, Chemistry and line emission from evolving Herbig Ae disks. *Astron. & Astrophys.* **463**, 203–216.
- Knapp, G. R. and M. Woodhams, 1993, Mass loss from cool supergiant stars.
- Kroeger, D., G. Hensler, and T. Freyer, 2006, Chemical self-enrichment of HII regions by the Wolf-Rayet phase of an 85 M_{\odot} star. *Astron. & Astrophys.* **450**, L5–L8.
- Krot, A. N., K. Nagashima, M. Bizzarro, G. R. Huss, A. M. Davis, B. S. Meyer, and A. A. Ulyanov, 2008, Multiple generations of refractory inclusions in the metal-rich carbonaceous chondrites Acfer 182/214 and Isheyevo. *Astrophys. J.* **672**, 713–721.
- Levison, H. F. and M. J. Duncan, 1997, From the Kuiper Belt to Jupiter-Family Comets: The Spatial Distribution of Ecliptic Comets. *Icarus* **127**, 13–32.
- Lewis, J. S., 1972, Low temperature condensation from the Solar nebula. *Icarus* **16**, 241.
- Lodders, K., 2004, Jupiter formed with more tar than ice. *Astrophys. J.* **611**, 587–597.
- Lodders, K., 2008, The solar argon abundance. *Astrophys. J.* **674**, 607–611.
- Lyons, J. R. and E. D. Young, 2005, CO self-shielding as the origin of oxygen isotope anomalies in the early solar nebula. *Nature* **435**, 317–320.
- Mabry, J. C., A. P. Meshik, C. M. Hohenberg, Y. Marrocchi, O. V. Pravdivtseva, R. C. Wiens, C. Olinger, D. B. Reisenfeld, J. Allton, R. Bastien, K. McNamara, E. Stansbery, and D. S. Burnett, 2007, Refinement and implications of noble gas measurements from Genesis. *LPSC* **38**, 2412.
- Mesa-Delgado, A., C. Esteban, and J. Garcia-Rojas, 2008, Small-scale behavior of the physical conditions and the abundance discrepancy in the Orion nebula. *Astrophys. J.* **675**, 389–404.

- Moeckel, N. and H. Throop, 2009, Bondi-Hoyle-Lyttleton accretion onto a protoplanetary disk. *Astrophys. J.* **707**, 268–277.
- Ouellette, N., S. J. Desch, and J. J. Hester, 2007, Interaction of supernova ejecta with nearby protoplanetary disks. *Astrophys. J.* **662**, 1268–1281.
- Owen, T. and T. Encrenaz, 2006, Compositional constraints on giant planet formation. *Plan. Spac. Sci.* **54**, 1188–1196.
- Owen, T., P. Mahaffy, H. B. Niemann, S. Atreya, T. Donahue, A. Bar-Nun, and I. de Pater, 1999, A low-temperature origin for the planetesimals that formed Jupiter. *Nature* **402**, 269–270.
- Ranen, M. C. and S. B. Jacobsen, 2006, Barium isotope heterogeneities in early solar system materials: applications to planetary reservoir models. *LPSC* **37**, 1832.
- Ranen, M. C. and S. B. Jacobsen, 2008, Three-component mixing in the protoplanetary disk: the isotopic evidence. *LPSC* **39**, 1954.
- Roulston, M. S. and D. J. Stevenson, 1995, Prediction of neon depletion in Jupiter’s atmosphere. *EOS* **76**, 343.
- Schaller, G., D. Schaerer, G. Meynet, and A. Maeder, 1992, New grids of stellar models from 0.8 to 120 Msol at $Z=0.020$ and $Z=0.001$. *Astron. & Astrophys. Suppl.* **96**, 269–331.
- Stasinska, G., G. Tenorio-Tagle, M. Rodriguez, and W. J. Henney, 2007, Enrichment of the interstellar medium by metal-rich droplets and the abundance bias in HII regions. *Astron. & Astrophys.* **471**, 193–204.
- Tachibana, S. and G. R. Huss, 2003, The initial abundances of ^{60}Fe in the solar system. *Astron. J.* **588**, L41–L44.

- Tenorio-Tagle, G., 1996, Interstellar matter hydrodynamics and the dispersal and mixing of heavy elements. *Astron. J.* **111**, 1641–1650.
- Throop, H. B. and J. Bally, 2008, Tail-end Bondi-Hoyle accretion in young star clusters: Implications for disks, stars, and planets. *Astron. J.* **135**, 2380–2397.
- Throop, H. B., J. Bally, L. W. Esposito, and M. J. McCaughrean, 2001, Evidence for dust grain growth in young circumstellar disks. *Science* **292**, 1686–1689.
- Trinquier, A., J.-L. Birck, and C. J. Allegre, 2007, Widespread ^{54}Cr heterogeneity in the inner solar system. *Astrophys. J.* **655**, 1179–1185.
- Tsamis, Y. G. and D. Pequignot, 2005, A photoionization-modelling study of 30 Doradus: the case for small-scale chemical inhomogeneity. *Month. Not. Royal Astron. Soc.* **364**, 687–704.
- Udry, S., D. Fischer, and D. Queloz, 2007, A decade of radial-velocity discoveries in the exoplanet domain. In *Protostars and Planets V*, 685–699, U. Ariz. Pr., Tucson.
- Villeneuve, J., M. Chaussidon, and G. Libourel, 2009, Homogeneous Distribution of ^{26}Al in the Solar System from the Mg Isotopic Composition of Chondrules. *Science* **325**, 985–988.
- Wang, L. and J. Hu, 1994, Blue-shifted oxygen lines and the clumpy ejecta of 1993J. *Nature* **369**, 380–382.
- Watson, A., K. R. Stapelfeldt, K. Wood, and F. Menard, 2007, Multi-wavelength imaging of young stellar object disks: toward an understanding of disk structure and dust grain evolution. In *Protostars and Planets V*, U. Ariz. Pr., Tucson.
- Weidenschilling, S. J., 1997, The origin of comets in the solar nebula: a unified model. *Icarus* **127**, 290–306.

- Wiens, R. C., D. S. Burnett, C. M. Hohenberg, A. Meshik, V. Heber, A. Grimberg, R. Wieler, and D. B. Reisenfeld, 2007, Solar and solar-wind composition results from the genesis mission. *Space Sci. Rev.* **130**, 161–171.
- Williams, B. J., K. J. Borkowski, S. P. Reynolds, J. C. Raymond, J. A. Morse, W. P. Blair, P. Chavamian, R. Sankrit, S. P. Hendrick, R. Chris Smith, S. Points, and P. F. Winkler, 2008, Ejecta, dust, and synchrotron radiation in B0540-69.3: A more Crab-like remnant than the Crab. *Astrophys. J.* **687**, 1054–1069.
- Wong, M. H., J. I. Lunine, S. K. Atreya, T. Johnson, P. R. Mahaffy, T. C. Owen, and T. Encrenaz, 2008, Oxygen and other volatiles in the giant planets and their satellites. 219–246.
- Woosley, S. E. and A. Heger, 2007, Nucleosynthesis and remnants in massive stars of solar metallicity. *Phys. Rep.* **442**, 269–283.
- Young, E. D., M. Gounelle, R. Smith, M. R. Morris, and K. M. Pontoppidan, 2008, Solar system oxygen isotope ratios result from pollution by Type II supernovae. *LPSC* **39**, 1329.
- Young, E. D., M. Gounelle, R. L. Smith, M. R. Morris, and K. M. Pontoppidan, 2009, The Oxygen Isotopic Composition of the Solar System in a Galactic Context: New Results for CO in Young Stellar Objects and Implications for the Birth Environment of the Solar System. *LPSC* **40**, 1967.
- Young, P. A. and C. L. Fryer, 2007, Uncertainties in supernova yields. I. One-dimensional explosions. *Astrophys. J.* **664**, 1033–1044.